Chemical Geology 374–375 (2014) 1–12

Contents lists available at ScienceDirect

Chemical Geology

journal homepage: www.elsevier.com/locate/chemgeo

Saharan aeolian input and effective humidity variations over western Europe during the Holocene from a high altitude record

F.J. Jiménez-Espejo [a,*], A. García-Alix [b], G. Jiménez-Moreno [c], M. Rodrigo-Gámiz [d], R.S. Anderson [e], F.J. Rodríguez-Tovar [c], F. Martínez-Ruiz [f], Santiago Giralt [g], A. Delgado Huertas [f], E. Pardo-Igúzquiza [h]

[a] Japan Agency for Marine-Earth Science and Technology, Yokosuka 237-0061, Japan
[b] Departamento de Didáctica de la Ciencias Experimentales, Universidad de Granada, Granada, Spain
[c] Departamento de Estratigrafía y Paleontología, Universidad de Granada, Granada, Spain
[d] NIOZ Royal Netherland Institute for Sea Research, Department of Marine Organic Biogeochemistry, Texel, The Netherlands
[e] School of Earth Sciences and Environmental Sustainability, Northern AZ University, USA
[f] Instituto Andaluz de Ciencias de la Tierra CSIC-UGR, Granada, Spain
[g] Institute of Earth Sciences Jaume Almera (CSIC), Lluís Solé i Sabarís s/n, 08028 Barcelona, Spain
[h] Instituto Geológico y Minero de España (IGME), Madrid, Spain

ARTICLE INFO

Article history:
Received 2 July 2013
Received in revised form 3 March 2014
Accepted 3 March 2014
Available online 13 March 2014

Editor: Michael E. Böttcher

Keywords:
Saharan dust
Holocene
South Iberia
Lacustrine record

ABSTRACT

Saharan dust inputs affect present day ecosystems and biogeochemical cycles at a global scale. Previous Saharan dust input reconstructions have been mainly based on marine records from the African margin, nevertheless dust reaching western-central Europe is mainly transported by high-altitude atmospheric currents and requires high altitude records for its reconstruction. The organic and inorganic geochemical study of sediments from a southern Iberia alpine lacustrine record has provided an exceptional reconstruction of Saharan dust impact and regional climatic variations during the Holocene. After the last deglaciation, results indicate that Saharan dust reached Western Europe in a stepwise fashion from 7.0 to 6.0 cal. kyr BP and increased since then until present, promoting major geochemical changes in the lacustrine system. Effective humidity reconstruction indicates wetter conditions during the early Holocene and progressive aridification during middle–late Holocene time, boosting abrupt changes in the lacustrine system. Cyclostratigraphic analyses and transport mechanisms both point to solar irradiance and aridity as major triggering factors for dust supply over Western Europe during the Holocene.

© 2014 Elsevier B.V. All rights reserved.

1. Introduction

Saharan–Sahel soil dust aerosols, exported to both Atlantic Ocean and Mediterranean regions, affect the biogeochemical and ecological cycles from oceans and continents and thus have an important impact on the global environment and human health (Moulin et al., 1997; Shinn et al., 2000; Goudie and Middleton, 2001; Griffin and Kellogg, 2004; Bonnet et al., 2005; Mush, 2013, among others). Due to its $CaCO_3$ content, Saharan dust significantly increases the pH of rain-water (Loÿe-Pilot et al., 1986) and influences the chemistry of soils and water masses over European regions (Goudie and Middleton, 2001; Waeles et al., 2007; Erel and Torrent, 2010). Paleo-dust deposition has been demonstrated to be a proxy for aridity (Petherick et al., 2009), climate variability (Jung et al., 2004), air mass circulation (Rohling et al., 2003) and wind strength (Mush, 2013). For this reason, understanding past evolution of Saharan dust deposition over Europe is vital to furthering our knowledge about present day ecosystems (Maher et al., 2010), and modern climate (e.g., Antón et al., 2012).

Remote alpine lakes are recognized as being very sensitive environments to aeolian input and climate changes (e.g., Adrian et al., 2009). The high biogeochemical sensitivity to Saharan aeolian dust has been previously documented in high-elevation alpine lakes of glacial origin from the southern Iberian Peninsula (e.g., Pulido-Villena et al., 2005; Morales-Baquero et al., 2006; Reche et al., 2009; Mladenov et al., 2011; Oliva and Gómez-Ortiz, 2012). The sensitivity of these lakes to external inputs, i.e., aeolian dust, pollutants and other aerosols, can be ascribed to their location at high altitudes (>3000 masl) above the tree line, thus being characterized by very small and poorly vegetated catchments. These lakes are located above the atmospheric boundary layer (>1500 masl) in the mainstream (1500–4000 masl) of Saharan dust transport (Talbot et al., 1986). Laguna de Rio Seco (LdRS), an alpine lake in Sierra Nevada located at the southern Iberia (Fig. 1), is one of these sites.

Abundances of specific major, minor and trace elements, combined with organic geochemical proxies have a great potential for reconstructing past depositional and environmental conditions (e.g., Blanchet et al., 2013). Nevertheless, the use of trace elements as geochemical proxies in lake sediments has not been fully exploited because each lacustrine system is a unique biogeochemical environment,

* Corresponding author.
E-mail address: fjjspejo@ugr.es (F.J. Jiménez-Espejo).

http://dx.doi.org/10.1016/j.chemgeo.2014.03.001
0009-2541/© 2014 Elsevier B.V. All rights reserved.

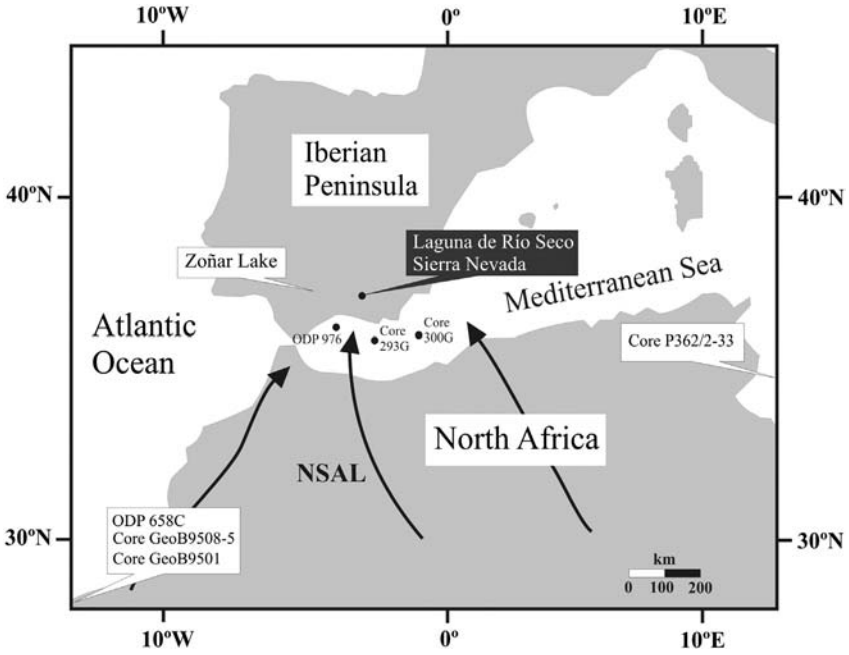

Fig. 1. Setting of Laguna de Río Seco (Sierra Nevada) in the Iberian Peninsula and other marine and terrestrial climate records discussed and located in nearby regions. Black arrows indicate the North Saharan Air Layers (NSAL) wind system.

making the interpretation very complex (Das et al., 2008). Element enrichment in shallow lake sediments is controlled by several factors, for example, terrigenous input, pH, phytoplankton abundance, and organic matter, among others (e.g., Bilali et al., 2002). Any fluctuation in these ruling factors can promote a series of geochemical processes, which affect the element accumulation. These geochemical changes can be preserved in peat and lacustrine records, allowing the reconstruction of past environmental conditions, in general, (Shotyk et al., 2002; Moreno et al., 2011; García-Alix et al., 2013) and dust input variations in particular (e.g., An et al., 2012; Allan et al., 2013).

Recently, an unprecedented pollen record in the South Iberian alpine region has been obtained from a sediment core recovered from LdRS (Anderson et al., 2011). Here we have studied this sediment record and analyzed a number of geochemical proxies in order to reconstruct regional water availability, effective humidity and aeolian input variations during the Holocene. The datasets were subjected to a detailed statistical analysis in order to identify their main sources and sedimentary processes ruling their temporal oscillations. Furthermore, cyclostratigraphic analyses were applied on the paleoclimate time series in order to identify periodicities and spectral signatures that might provide insights on the major forcing mechanisms that triggered climate periods of aeolian dust deposition and regional water availability over Western Europe.

2. Methods

2.1. Geographical context, core location, age model and sampling

Sierra Nevada is the highest mountain range located in the Iberian Peninsula. During the Late Pleistocene numerous depressions formed through glacial erosion between 2600 and 3100 masl in this mountain range. Later on, during the deglaciation, small lakes developed (Schulte, 2002). LdRS (37° 02.43′ N, 3° 20.57′ W) is one of these glacial lakes located at ~3020 masl, with a surface of 0.42 ha and a maximum depth of ~2 m (Morales-Baquero et al., 1999) (Fig. 1). It is placed in a south-facing cirque, and its catchment, constituted by a siliceous mica schist substrate, is reduced to about 9.9 ha (Morales-Baquero et al., 1999). This lake is covered in snow most of the year, with the snow free period typically occurring from June to October.

LdRS is an oligotrophic lake with a significant influence of Saharan dust inputs on present day lake biogeochemistry (Morales-Baquero et al., 2006; Pulido-Villena et al., 2006; Reche et al., 2009). A 150 cm-long sediment core was collected in September 2006 from the center of LdRS (Fig. 1). The core lithology of the uppermost 133 cm is characterized by banded peaty and silty clays whereas the lowermost 17 cm corresponds to bluish-gray glacial clay and gravels (Anderson et al., 2011). The age model applied in this study follows Anderson et al. (2011) and it is based on 9 calibrated AMS radiocarbon dates using CALIB 5.0.2 (Stuiver et al., 1998). The age of the intermediate samples has been calculated by linear interpolation. Sediment accumulation rates (SAR) are described in Anderson et al. (2011) and vary between 0.13 cm/yr above 15 cm and 0.007–0.0063 cm/yr below 15 cm. The average SAR for the whole record is 0.013 cm/yr. The sedimentary record of this lake continuously covers most of the Holocene, from ~11 cal. kyr BP to present (Anderson et al., 2011).

2.2. Sample preparation and statistical analysis

Carbon stable isotopes, atomic C/N ratios and major and trace elements were analyzed from 68 sediment samples, taken at ~2-cm intervals (an average of ca. 165 years between samples) in the 133 cm upper part of the sediment core. For the isotopic analyses of the organic matter, samples were decalcified with 1:1 HCl in order to eliminate the carbonate fraction. Carbon isotopes ($\delta^{13}C$), and the atomic C/N ratios were measured by means of an elemental analyser (Carlo Erba Ba 1500 series 2) connected to a Thermo Finnigan DELTAplus XL mass spectrometer. Samples were measured in duplicate. The carbon isotopic composition of the studied samples were specified by two internal standards with values of −30.63‰ and −11.65‰ (V-PDB), contrasted with the IAEA international references NBS-22, IAEA-CH-7, and IAEA-CH-6. Carbon isotope results are expressed in δ notation, using the standard V-PDB. The calculated precision, after correction for mass spectrometer daily drift, using standards systematically interspersed in analytical batches, was better than ±0.1‰ for $\delta^{13}C$.

Major element measurements (Mg, Al, Ca, Mn and Fe) were obtained by atomic absorption spectrometry (AAS) using a Perkin-Elmer 5100 spectrometer with an analytic error of 2%. Trace element analyses (Sc, V, Cr, Co, Ni, Cu, Zn, Ga, Y, Nb, Ta, Zr, Hf, Mo, Sn, Tl, Pb, U, Th, La and Lu)

were performed using Inductively Coupled Plasma–Mass Spectrometry (ICP–MS) after HNO_3 (65% Panreac PA-AR) + HF (40% Suprapur) digestion of 0.1004 to 0.1008 g of sample powder in a Teflon-lined vessel for 150 min at high temperature and pressure, evaporation to dryness, and subsequent dissolution in 100 ml of 4 vol.% HNO_3. Measurements were taken in triplicate through spectrometry (Perkin Elmer Sciex Elan 5000) using Re and Rh (25 ppb) as internal standards. Data were contrasted with the following reference geostandards: UBN, PMS, WSE, BEN, BR, AGV, DRN, GSN GA and GH (Govindaraju, 1994). The instrumental error is ±2% for elemental concentrations <50 ppm and ±5% for concentrations between 50 to 5 ppm respectively (Bea, 1996).

Statistical treatment of analytical data was performed using the software package R (Development Core Team, 2013). Stratigraphically-constrained cluster analyses were applied to identify the periods with homogeneous geochemical behavior and the outliers (isolated samples with anomalous values) (Fig. 2). The normalized geochemical dataset was also clustered. For this purpose, unconstrained hierarchical cluster analysis was also applied on the dataset in order to determine the main geochemical families (Fig. 3). Approximately unbiased (au) p-value and bootstrap probability (bp) value were calculated to establish the significant clusters. This second cluster analysis was calculated to establish the significant clusters and calculated using the pvclust R package (Suzuki and Shimodaira, 2011). The complete linkage method (or furthest neighbor method) was used for clustering purposes. Pearson's r correlation index and their significance (p-value) have been calculated for the complete geochemical dataset.

Cyclostratigraphic analysis of the time series from the different proxies has been conducted with the Lomb–Scargle periodogram (Lomb, 1976; Scargle, 1982) (see Supplementary information). This is a very appropriate spectral methodology when working with uneven sampling data, as in our case study (Rodríguez-Tovar et al., 2010; Pardo-Igúzquiza and Rodríguez-Tovar, 2012). The power spectrum has been estimated, by the Lomb–Scargle periodogram, on a frequency range of [0, 0.007] with a frequency interval of 0.000014 cycles per year. That is, the range

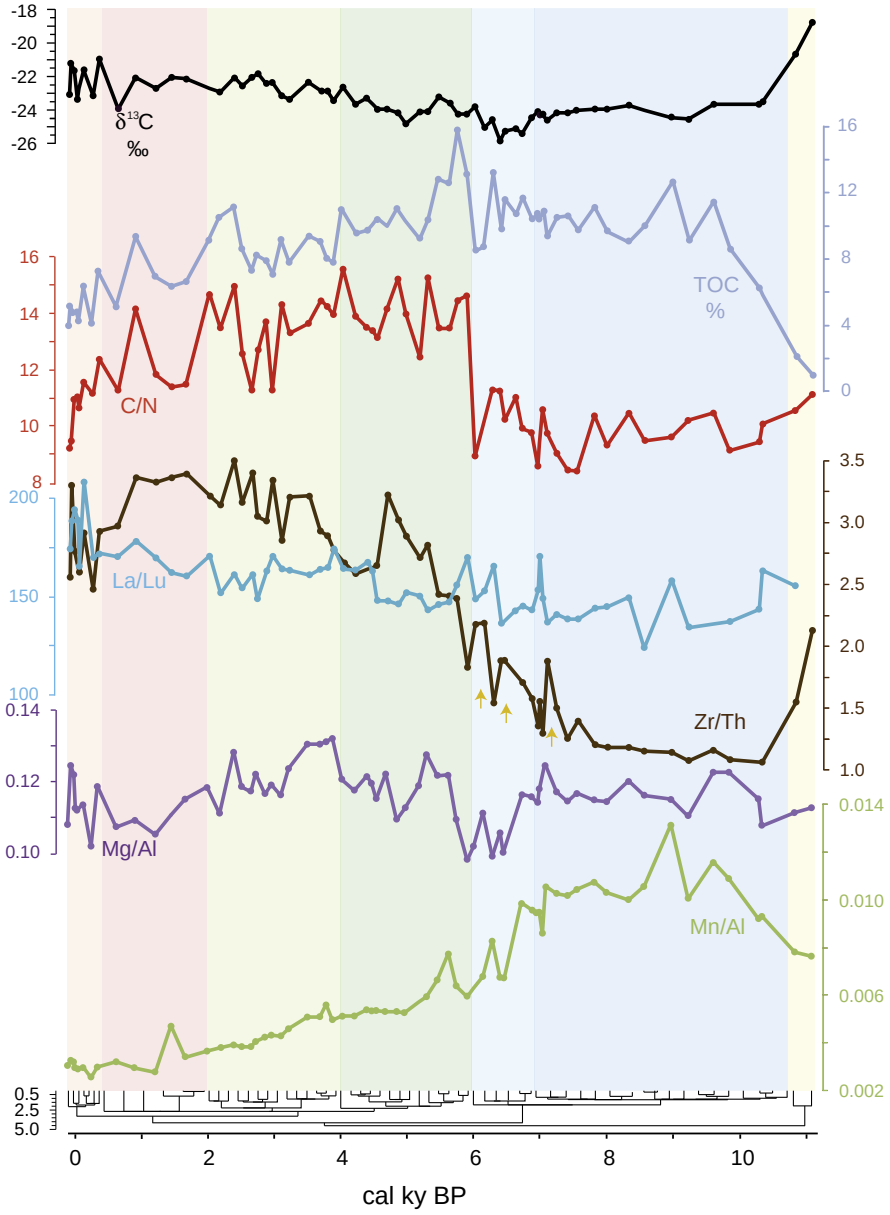

Fig. 2. Age profile of organic matter $\delta^{13}C$, total organic content (TOC) (%), Carbon/Nitrogen (C/N), Zr/Th, La/Lu, Mg/Al and Mn/Al ($\times 10^3$) ratios measured at Laguna de Río Seco. Colored bars represent the different seven consecutive environmental phases obtained from the stratigraphically constrained cluster analyses on $\delta^{13}C$, C/N atomic ratio, and Mn/Al, Mg/Al, La/Lu and Zr/Th. Orange arrows represent earliest dust input to the lake. (For interpretation of the references to color in this figure, the reader is referred to the web version of this article.)

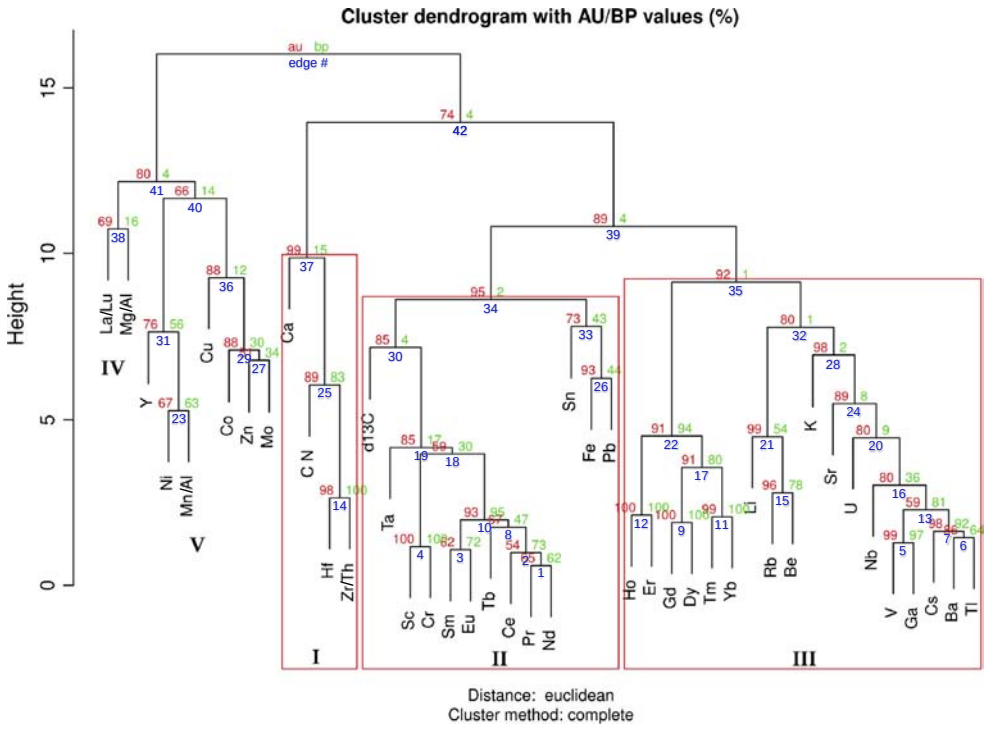

Fig. 3. Unconstrained hierarchical cluster analysis of the geochemical data. Approximately unbiased (au) p-value (in red) and bootstrap probability (bp) value (in green) allowed us to identify the significant clusters. The pvclust R package was employed for this purpose (Suzuki and Shimodaira, 2011). Clusters significant at 0.90 have been highlighted by red boxes. Roman numerals indicate main geochemical families. (For interpretation of the references to color in this figure, the reader is referred to the web version of this article.)

of frequencies that has been analyzed, searching for hidden periodicities, is [0, 0.007]. This interval is analyzed at discrete frequencies equal to k0.000014 being k an integer from 1 to 2000.

The estimated periodogram is then smoothed with a linear filter of 21 terms. The uncertainty is evaluated by the permutation test, which takes into account all these parameters. To evaluate the significance of the registered spectral peaks, one appropriate method is the implemented achieved significance level (ACL) using the permutation test (see Pardo-Igúzquiza and Rodríguez-Tovar, 2000, for a detailed description). According to this, the obtained peaks in the ACL can be considered as primary, and not secondarily generated by the applied methodology; from all the peaks registered with the Lomb–Scargle only those also registered in the ACL have been interpreted.

To adopt a conservative position, we only consider those cycles in the frequency range with more possibilities of being registered, discarding those on the edge of the low frequencies close to the vertical axe in the ACL, as well as those corresponding to thickness close to the sampling interval. Thus, taking into account that the studied part of the sediment core spans around 11,100 yr, those cycles at the lowest

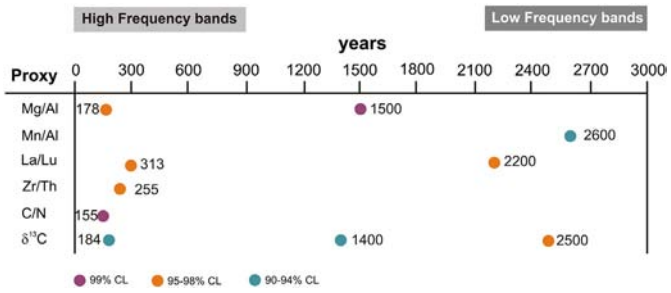

Fig. 4. Spectral peaks summary obtained with the spectral method at high and low frequency bands. Color in dots defines the confidential level (%) obtained. Power spectra plots are available in Supplementary Information. (For interpretation of the references to color in this figure, the reader is referred to the web version of this article.)

frequencies calibrated as higher than 3500 yr, have not been considered. Moreover, according to the estimated time represented for the sampling interval (around 160 yr), those cycles in the highest frequency band, calibrated as lower than 320 yr, were also not interpreted. Thus, we have only considered those cycles registered in the frequency band corresponding to periodicities between 320 and 3500 yr (Fig. 4 and Supplementary information).

2.3. Selected proxies interpretation and corrections

In the last decades inorganic chemical proxies has been demonstrated to be an extremely useful tool for paleoenviromental reconstructions (e.g., Calvert and Pedersen, 2007). The use of several element ratios in order to define changes in the terrigenous/biological composition is based on the relationship between different minerals and their sources. Nevertheless, the interpretation of chemical facies/ratios as response to environmental changes has to be done carefully, as similar element response can be obtained through different environmental forcings, such as aridity, anoxia, productivity, antrophic influence, or change in mineral sources, among others.

The first correction that should be done is related to dilution effect promoted by mineral phases of biogenic origin, commonly calcium carbonate and opal. Thus, to compare major and trace element proportions in samples with variable carbonate and opal contents, it is common to normalize absolute trace-element concentrations to Al, Ti or Th, assuming a unique detrital origin for these elements (e.g., Brumsack, 1986; Calvert and Pedersen, 1993; Piper and Calvert, 2009). Al normalization has some drawbacks that are most likely to occur when the coefficient of variation (i.e. the standard deviation divided by the mean) of the Al concentration is large compared to the coefficient of variation of the other elements (Van der Weijden, 2002). However, the coefficient of variation in this record is low 0.17 for Al, 0.4 for Zr and 0.29 for Mn.

We selected diverse elemental ratios as most representative for aeolian (Zr/Th), source composition (La/Lu), redox (Mn/Al) and detrital (Mg/Al) proxies. The selection was done based on previous data, on

the composition of the catchment, dust input mineralogy and on the correlation between different elements (Supplementary information). The selected aeolian proxy is the Zr/Th ratio because Saharan dust is enriched in heavy minerals such as zircon (e.g., Moreno et al., 2006; Hemming, 2007; Aarons et al., 2013; Scheuvens et al., 2013). In this sense the Zr/Th, or the equivalent Zr/Al ratio, has been extensively used as a proxy of aeolian input in the Mediterranean, Atlantic and also Caribbean regions (Mahowald et al., 2002; Cole et al., 2009; Rodrigo-Gámiz et al., 2011). The La/Lu ratio represents the whole Rare Earth Elements (REE) pattern and allows to discriminate between relative felsic and basaltic input in dust source signatures (Rollinson, 1993). The La/Lu ratio appears to be a reliable fingerprint for Saharan dust input in the Mediterranean area (Wehausen and Brumsack, 1999; Martínez-Ruiz et al., 2000) and other regions (Marx et al., 2011). In this way, the La/Lu ratio has been specifically used to discriminate aeolian inputs originating from the African craton (Hamroush and Stanley, 1990; Moreno et al., 2006; Castillo et al., 2008; Mush et al., 2010). In close marine and coastal areas La/Lu ratio range between 100 during humid period to >150 during Pleistocene and Holocene arid periods when African dust material has been described (Gallego-Torres et al., 2007; Cortés-Sánchez et al., 2011). In very small catchments as the LdRS, which is mainly composed of metamorphic rocks, the arrival of a distantly sourced dust signature can be easily recognized by changes in this ratio.

The manganese is a solid phase electron acceptor that reflects paleoredox conditions in lacustrine systems (Richardson and Nealson, 1989; Eusterhues et al., 2005; Jouve et al., 2013; Naeher et al., 2013). Mn precipitates out in sediment mainly as Mn^{4+}, usually as oxides, and re-solubilizes in the water column mainly as Mn^{2+} (Richardson and Nealson, 1989). Nevertheless, precipitated manganese can be newly dissolved linking the preservation of Mn/Al ratio enrichments to sedimentation rates and pore water geochemistry (Och et al., 2012). At LdRS, Mn/Al shows a high correlation with previously described effective humidity proxies – e.g. the occurrence of *Betula*, *Pinus* and *Artemisia* pollen (Anderson et al., 2011) – and marked diagenetic peaks are absent (Mangini et al., 2001) pointing to a good preservation for the Mn record with a limited diagenetic overprint. This relationship between Mn content and effective humidity can be explained by the presence of reducing conditions in the lake bottom and corresponding chemocline promoting an enrichment in Mn during humid periods (Mackereth, 1966; Schaller and Wehrli, 1996). Mn precipitation also can be furthermore catalyzed by Mn oxidizing bacteria (Diem and Stumn, 1984).

LdRS catchment is composed by metamorphic quartzites, schist and mica-schist, and Mg-bearing carbonates are almost absent (Castillo Martín, 2009). In this scenario Mg-chlorites, measured in the clay mineral fraction, could be the main sources for Mg content. The high correlation ($r > 0.75$) between Mg and other typical alumino-silicates elements (e.g., K, Al, Th) also supports this detrital origin (Supplementary information). An increase in Mg respective to other detrital elements can be interpreted as an enrichment in Mg-chlorite (clay mineral) input respect to other phases. A hydrodynamic process, like an increase in surface runoff during humid periods, could explain this mineralogical sorting (Mathews, 1956) as observed in marine depositional environments (e.g., Jiménez-Espejo et al., 2007a).

3. Results

3.1. Organic and inorganic geochemistry

Results are described using a stratigraphically constrained cluster analysis (Fig. 2) based on $\delta^{13}C$, C/N atomic ratio, and Mn/Al, Mg/Al, La/Lu and Zr/Th ratios. Seven main phases in the studied record can be observed (Fig. 2).

Phase 1 (between 11.1 and 10.5 cal. kyr BP): this phase is impoverished in organic carbon (TOC < 2.1%). This period is characterized by the highest $\delta^{13}C$ values ($-19.7 \pm 1.3‰$) and the C/N atomic ratio has a mean value of 10.9 ± 0.4. Minor changes in the inorganic ratios are observed except for the Zr/Th (Fig. 2).

Phase 2 (between ~10.5 and ~6.9 cal. kyr BP): TOC values increased ($9.8 \pm 1.7\%$), however $\delta^{13}C$ values ($24.0 \pm 0.3‰$) and C/N atomic ratio (9.6 ± 0.7) decreased (Fig. 2). All the inorganic proxies shared a flat pattern. The Zr/Th ratio displayed a progressive increase from ~7.6 cal. kyr BP onwards (Fig. 2).

Phase 3 (between ~6.9 and ~6.0 cal. kyr BP): this phase represented a disruption in the studied proxies. TOC values were high ($10.6 \pm 1.7\%$), $\delta^{13}C$ values slightly decreased ($-25‰ \pm 0.7‰$), and C/N atomic ratio oscillated around 10. The Mg/Al ratio showed the lowest values (<0.1). The La/Lu ratio was characterized by variations from ~165 to ~135. Zr content increased remarkably and Mn/Al ratio showed an opposite trend.

Phase 4 (between ~6.0 and ~4.0 cal. kyr BP): this phase is characterized by rising upwards TOC (up to $11.2 \pm 1.8\%$) and $\delta^{13}C$ ($-23.8 \pm 0.5‰$) values, and the C/N atomic ratio was always above 10 (14 ± 0.9). Zr/Th shows a major peak at 4.7 cal. kyr BP, with an opposite trend when compared with the Mg/Al ratio. La/Lu and Mn/Al ratios were characterized by a flat and stable pattern during this interval.

Phase 5 (between ~4.0 and 2.0 cal. kyr BP): TOC values decreased to around 9, as well as the $\delta^{13}C$ ($-22.6 \pm 0.5‰$), and the C/N atomic ratios (13.5 ± 1.2). Since ~4.4 cal. kyr BP, the La/Lu ratio achieved constant high values (with average around 155), only reached punctually during previous Holocene periods. Zr/Th showed an increasing trend with a seesaw pattern and the Mn/Al again displayed an opposite trend. Mg/Al and La/Lu ratios depicted no clear trends during this interval.

Phase 6 (between ~2.0 and 0.4 cal. kyr BP) seems to be a continuation of the previous phase, although with more attenuated trends. TOC values decreased ($6.9 \pm 1.4\%$), as well as $\delta^{13}C$ ($-22.3 \pm 1.0‰$) and C/N atomic ratio (12.1 ± 1.1).

Phase 7 (last 400 cal. yr BP) showed significant changes in the proxy data when compared with previous periods. TOC values dropped ($4.8 \pm 0.8\%$), and the C/N atomic ratio oscillated around 10 (10.6 ± 0.9). Zr/Th and La/Lu ratios showed abrupt increases reaching highest values for the entire Holocene, and Mg/Al was relatively low.

3.2. Statistical approach

Statistical correlations (Pearson's r) and significance (p-values) as well as stratigraphically unconstrained hierarchical cluster analysis were calculated using all proxies and representative ratios to highlight the main environmental and climate processes underlying these datasets (see Supplementary information). The chemical elements can be grouped according to their chemical affinity (Fig. 3). The first group is composed by chemical elements related to the eolian (Zr/Th) input like Ca and Hf. The C/N ratio is also associated with this eolian terrigenous material owing to increases in the lake productivity that are due to the input of Saharan dust. TOC shows same C/N ratio pattern and not represented because reiterative. The second group is made up of chemical elements related to metallic-rich sediments (Ta, Sc, Cr, Sm, Eu, Tb, Ce, Pr, Nd, Fe, Sn and Pb) whereas the third group is composed of the chemical elements that are present in clays, either in their structure or adsorbed in between their octaedrical layers (K, Sr, U, Nb, V, Ga, Cs, Ba, Tl, Li, Rb, Be, Ho, Er, Gd, Dy, Tm and Yb). The fifth group includes the chemical elements that are sensitive to redox changes (Cu, Co, Zn, Mo, Ni, Y and the Mn/Al ratio). The La/Lu and Mg/Al ratios also are grouped but with a clusters significant at 0.80.

3.3. Cyclostratigraphy

The results obtained from the cyclostratigraphic analysis allow the differentiation of cycles in the low-frequency bands at 2600–2200 yr and 1500–1400 yr, and in the high-frequency ones at 313 yr and 256 yr (Fig. 4). Used methodology and the uneven sample resolution allow us

to recognize centennial-scale cycles but average sample resolution indicates that they must be considered with caution, thus only millennial-scale cycles are considered in this study.

The 2600–2200 yr cycle is the most frequently registered, being observed in three of the studied proxies, La/Lu, Mn/Al, and $\delta^{13}C$ (95–99% CL). The 1500–1400 yr cycle is registered in Mg/Al and $\delta^{13}C$, with special high significance (99% CL) in the Mg/Al.

4. Discussion

4.1. Saharan aeolian input signal and evolution during the Holocene

The study of Saharan dust input over the African margin during the Holocene shows paradoxical situations, like high dust input to the North Canary basin (approx. 32°N) during the early-middle Holocene (Moreno et al., 2001; Bozzano et al., 2002) and high dust input in southern locations (approx. 22°N) during middle–late Holocene (Adkins et al., 2006). Our data from LdRS indicate that lake sedimentation was characterized by enhanced supply of Saharan dust during early Holocene around 11 cal. kyr BP, and more recently at 7.1, 6.4 and 6.2 cal. kyr BP (Fig. 2 orange arrows), with a progressive increase from 6.0 cal. kyr BP, with relative decrease at 4.2 kyr and between 1.0 and 0.2 cal. kyr BP. An increase in Saharan dust input pulses or decrease in fluvial detrital input using a variety of proxies (grain size, plant wax *n*-alkanes, K/Al ratio) has been previously described in the western and eastern Mediterranean and off-shore NW Africa marine records at 7.4 cal. kyr BP and a dry pulse has been recognized in northern Africa between 8.5 and 7.3 cal. kyr BP (Fig. 5) (Petit-Maire and Guo, 1996; Jiménez-Espejo et al., 2007b; Niedermeyer et al., 2010; Rodrigo-Gámiz et al., 2011; Cortés Sánchez et al., 2012; Blanchet et al., 2013). The timing of the "African Humid Period" (AHP) demise has been estimated between 6.0 and 4.2 cal. kyr BP, and its end is described as abrupt (deMenocal et al., 2000; Cole et al., 2009) or progressive (Jung et al., 2004; Lézine, 2009; Marshall et al., 2011; Blanchet et al., 2013) depending on the record and its location. In our case, the first evidence of aeolian dust input at LdRS, related with the AHP demise, is recorded around 7.0 cal. kyr BP with an increasing trend in the Zr/Th ratio and *Artemisia* pollen and a decrease in *Betula* and *Pinus* pollen percentages (Fig. 5 e, f, h, i). That could be related to the fact that aridity of the source region is a necessary condition for dust availability, but storminess and air turbulence are also needed to uplift dust and inject it into the troposphere (Bozzano et al., 2002; Hodell et al., 2013). Our data indicate that these specifically required arid and atmospheric configurations were punctually established from 7.0 to 6.1 cal. kyr BP, and persistently occurred from 6.0 cal. kyr BP until present. At 7.0 cal. kyr BP a drastic decrease of lake levels in the Sahara–Sahel belt took place (Liu et al., 2007 and reference therein), and dry lake basins are major components of Saharan dust (Moreno et al., 2006). The onset of the persistent conditions coincides with the Mid-Holocene transitional character when global climate forcing started to change (Debret et al., 2009) and the transition between mainly humid to mainly arid conditions was recognized in the entire Mediterranean basin (Jalut et al., 2011; Rodrigo-Gámiz et al., 2011). This aridification has been linked with >5° latitudinal southward migration of the ITCZ (Arbuszewski et al., 2013).

In addition, signatures of the most recent changes in the Saharan environment and Saharan dust composition also appear to be recognized at LdRS. Peaks in the Zr/Th ratio are broadly synchronous with the La/Lu ratio in the LdRS record but they differ in orientation and intensity during the Holocene (Fig. 2). This could be related to changes in the average composition of the aeolian dust (Moreno et al., 2006; Pey et al., 2009). In addition, dust deposition increased in the last 200 years due to the onset of commercial agriculture in the Sahel region (Mulitza et al., 2010). In the LdRS record we observed an increase in the Zr/Th ratio and unusually high La/Lu ratio, pointing to a marked change in the origin and/or composition of the dust reaching southern Iberia (Fig. 5e). This increase in the La/Lu ratios indicating more La content could reflect enhanced granitic weathered material from the West African craton in agreement with present day Saharan dust provenance region (Cole et al., 2009; Skonieczny et al., 2013). Nevertheless, effects of local anthropogenic impact cannot be discarded.

4.2. External input, regional productivity and effective humidity

LdRS is at present a small oligotrophic lake where biogeochemical cycles are highly influenced by the effect of Saharan dust deposition (Pulido-Villena et al., 2005; Morales-Baquero et al., 2006; Reche et al., 2009). Although the C/N atomic ratio indicates that the organic matter has a mixed aquatic (algal)/continental origin in the LdRS, the low C/N ratio, which in some cases is around 10 or lower (Fig. 2) suggests a significant contribution from an algal source (according to Meyers et al., 1994; Meyers and Teranes, 2001; among others), especially between ~10 and ~6 cal. kyr BP (Fig. 2), in agreement with wetter conditions in the alpine lakes from Sierra Nevada (Anderson et al., 2011; García-Alix et al., 2012; Jiménez Moreno and Anderson, 2012).

4.2.1. Early Holocene glacial input and humid conditions (~11.1–6.0 cal. kyr BP)

Anderson et al. (2011) suggested that the highest percentage of *Botryococcus* colonies that occurred during the first part of the record (~11.1–10.5 cal kyr BP) pointed to either relatively high lake water levels or perhaps to a wash out of nutrients during deglaciation. Pollen and geochemical marine records in the Iberian Mediterranean indicate an aridification episode during this time interval (Fletcher and Sanchez-Goñi, 2008; Rodrigo-Gámiz et al., 2011; Bellin et al., 2013), making improbable high lake levels by precipitation. Our record also indicates arid conditions with high Zr and *Artemisia* contents (Fig. 5e, f) (Anderson et al., 2011), but it is remarkable that the highest $\delta^{13}C$ – −18‰ – is also reached during this interval (Fig. 2). This is a typical value for organic matter composed by remains from soil and C4 plants (Eglinton et al., 2002). The most plausible explanation for all these observations is a mixed input coming both from the atmosphere and from melting glaciers. Both ice and rock glaciers existed in Sierra Nevada during the preceding Younger Dryas cold period, becoming significantly diminished around 10.5 ± 0.3 cal. kyr BP (Palade et al., 2011). This melt water could have contributed to the lacustrine system with "old carbon" (derived from C4 plant remains) and additional Zr input coming from the Sahara that accumulated during the Younger Dryas on the glacier. This fact, together with the absence of evidence of C4 plants in this area at that time (Ortiz et al., 2004, 2010), could explain the high $\delta^{13}C$ values in the sediments during the initial stage of the record. Therefore, despite the generally arid conditions that could have prevailed during this early stage, dust and other nutrients from melting glaciers most likely reached LdRS, probably enriching the lacustrine system and promoting high lacustrine levels.

The period from ~10.5 to ~6.1 cal. kyr BP is generally characterized by relatively low C/N atomic ratio (~10), high TOC content and Mn/Al ratio, and low $\delta^{13}C$ values (Figs. 2 and 5g). Palynological data also show relative high abundance of algae (*Botryococcus* and *Pediastrum*), ferns (*Botrychium*), aquatic plants (*Potamogeton* and Cyperaceae), *Pinus* and temperate mesic trees (*Betula* and deciduous *Quercus*), during this period (Anderson et al., 2011; Jimenez-Moreno and Anderson, 2012). All these proxies suggest relatively higher humidity conditions than today and the maximum development of the lacustrine system. The low C/N atomic ratio suggests a large contribution of algal organic matter (OM) to the sediment (Meyers, 1994; Meyers and Teranes, 2001; among others), and for periods when the C/N atomic ratio dropped below 10 it was the most important contributor of OM to the lake.

The high Mn/Al ratios obtained from the LdRS record at this time could be related to more dysoxic conditions on the lake bottom (e.g., Eusterhues et al., 2005; Jouve et al., 2013; Naeher et al., 2013). Despite

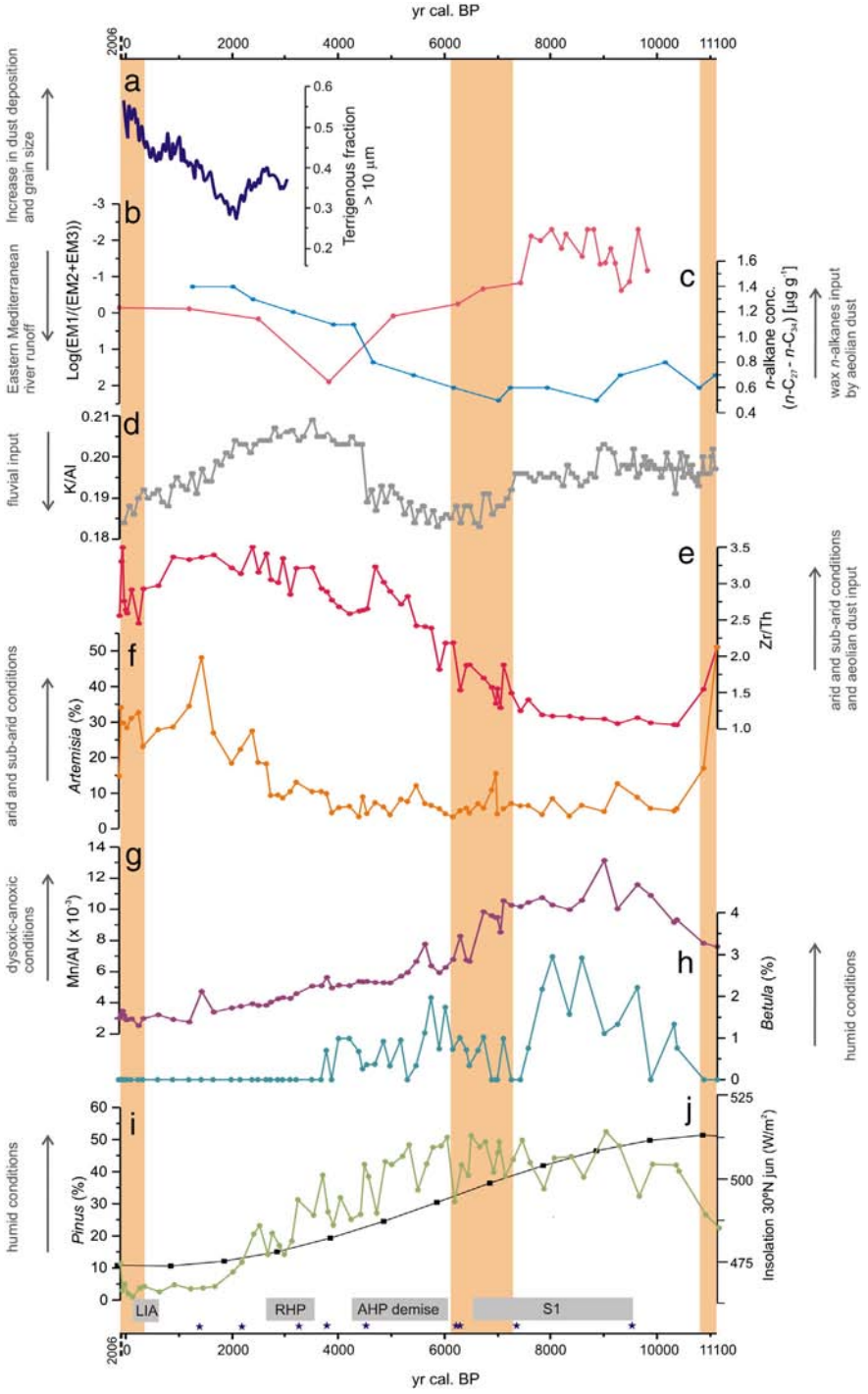

Fig. 5. Age profiles of Zr/Th (e) and Mn/Al ($\times 10^3$) (g) ratios in Laguna de Río Seco compared with selected organic and inorganic proxies from different records located in the Mediterranean and North African regions. From the top to the bottom: a) terrigenous grain-size fraction (>10 μm) (Mulitza et al., 2010); b) EM1/(EM2 + EM3) ratio used as fluvial/aeolian contribution to the terrigenous fraction in the eastern Mediterranean (Blanchet et al., 2013); c) wax *n*-alkane concentration (n-C_{27}–n-C_{34}) [μg g^{-1}] (Niedermeyer et al., 2010); d) fluvial-derived input ratio in the westernmost Mediterranean (Rodrigo-Gámiz et al., 2011); f, h, i) pollen percentages of *Artemisia*, *Betula*, and *Pinus* in LdRS (Anderson et al., 2011); j) summer insolation curve (June) at 30°N (Berger and Loutre, 1991). Stars show dated samples. Orange bars highlight main discussed intervals. Gray bars indicate time interval for the Sapropel 1 desposition (S1), the African Humid Period demise (AHP), the Roman Humid Period (RHP) and the Little Ice Age nLIA). (For interpretation of the references to color in this figure, the reader is referred to the web version of this article.)

the fact that shallow lakes typically remain well-oxygenated throughout the year (e.g., Elbaz-Poulichet et al., 1997) one plausible explanation for this could be that during this humid period algae and bacteria productivity was high. This, together with abundant external input (nutrients), could have promoted low C/N and high OM content. Our explanation is supported by presumed immature soil development covering the metamorphic bedrock, which probably limited the terrestrial vascular plant communities, thus exporting terrestrially-derived carbon to the lacustrine sediments. Thus, the high effective humidity and higher organic matter content caused low oxygenation and high Mn content.

The arrival of Saharan dust is newly recorded in the LdRS at 7.0 cal. kyr BP (Fig. 2). This promoted major changes in the LdRS biogeochemistry, for example, a decrease in the Mn/Al ratio, abrupt oscillations

in the C/N atomic ratio (fast increase/decrease) and heavier $\delta^{13}C$ values. This indicates that Saharan dust input affected the LdRS ventilation and increased productivity, probably due to the supply of carbonates and other nutrients to the lake. Aeolian dust input is the only natural supply of calcium carbonate into the lake, as siliceous rocks compose the catchment at LdRS (Pulido-Villena et al., 2006). The increase in aeolian input 7.0 cal. kyr BP (Zr/Th ratio) is supported by a regional decrease in effective humidity (*Pinus* and mesic tree content) from LdRS and the nearby Borreguiles de la Virgen records (Figs. 5e, h and i) (Anderson et al., 2011; Jiménez-Moreno and Anderson, 2012). A similar aridification trend can be found in other parts of the Iberian Peninsula (e.g., Jalut et al, 2000; Carrión, 2002; Carrión et al., 2003; Morellón et al., 2009; Morales-Molino et al., 2013), the Italian Peninsula (Sadori and Narcisi, 2001), the Peloponese (Jahns, 1993) and Sahara region (Liu et al., 2007).

At the end of this period (between ~6.8 and 6.0 cal. kyr BP) there is a slight increase in C/N and Zr/Al ratios, coupled with a decrease in the $\delta^{13}C$ value, mesic arboreal trees and *Pinus* percentages, and Mg/Al and Mn/Al ratios (Figs. 2 and 5). Although OM derived from algae continued to be important (C/N atomic ratio above 10), an increase in land plant contribution to the lake is apparent at this time. This can be interpreted as a transitional stage with relatively less humid conditions and a progressive increase in aeolian dust into LdRS. A progressive increase in the signal of aridity beginning ca. 7.0 cal. kyr BP has also been observed in another Sierra Nevada alpine site, i.e. Borreguiles de la Virgen (García-Alix et al., 2012; Jiménez-Moreno et al., 2013).

4.2.2. Middle-Late Holocene arid conditions (last ~6.0 cal kyr BP)

An abrupt increase in the C/N atomic ratio occurred in the LdRS lake record at ~6.0 cal. kyr BP. This is related to a substantial change in the main OM contribution in the lake from mostly algal to a more vascular plant input. This probably points to a major change in the lake that triggered the decrease in algal production at that time, most likely a drop in lake level due to an increased aridity. This is paralleled simultaneously by a progressive increase in $\delta^{13}C$ that may also be interpreted as a progressive aridification trend, perhaps related to a better water-use efficiency in vascular plants during dry conditions (Farquhar et al., 1982), together with a biogeochemical response of the lacustrine production to aeolian Saharan inputs with heavier $\delta^{13}C$ values. The inorganic geochemical proxies analyzed here also agree with this progressive aridification trend (Figs. 2 and 5). The Zr/Th ratio shows enhanced Saharan dust deposition in the lake since ~6.0 cal. kyr BP, which parallels other records from Mediterranean basins and North Africa offshore (Neidermeyer et al., 2010; Rodrigo-Gámiz et al., 2011; Blanchet et al., 2013).

Mn/Al ratio shows an opposite trend that can be interpreted as a progressive decrease in algal-bacterial productivity due to lowered lake water level. However, a relative maximum was reached at 5.5 cal. kyr BP (Fig. 5g). This Mn enrichment is concurrent with a humid pulse recognized in other records around the western Mediterranean, for instance, in Sicily (e.g., Sadori and Narcisi, 2001).

Besides this progressive trend, the Zr/Th ratio also shows relative decrease in dust deposition between 4.5 and 4.0 cal. kyr BP and between 2.2 and 2.0 cal. kyr BP. The first decrease is coincident with the major arid event recognized at 4200 cal. years BP in the Italian Peninsula (Drysdale et al., 2006), the Levant (Bar-Matthews et al., 2003), and North and central Africa (Guo et al., 2000; Thompson et al., 2002) among other locations. At LdRS effective humidity proxies (Mg/Al and C/N ratios and *Pinus* percentages) indicate certain aridification. This uncoupling between regional effective humidity proxies and aeolian dust could be related to migrations of the summer convective system and the North Saharan Air Layers (NSAL) trajectories as described during previous Holocene periods (Trauth et al., 2009). Probably the foremost reason for these patterns is that regional and temporal character of the effects of solar forcing results in local or regional redistribution of climatic patterns and their local amplitude, as previously described in the Mediterranean region (Versteegh et al., 2007). The second decrease in Zr/Th, at 2.2–2.0 cal. kyr BP, is roughly coincident with high precipitation levels in Southern Iberia, the called Humid Ibero–Roman period (Martin-Puertas et al., 2010; Nieto-Moreno et al., 2011), and Sicily (Sadori et al., 2013), among other locations. Other effective humidity proxies at LdRS (Mg/Al, TOC% and C/N) show a more clear increase timing coincidence to the Ibero–Roman period, indicating again the complex relationship between Saharan dust amount reaching this site and regional effective humidity.

Major changes in dust deposition and lacustrine environment in the LdRS occurred during the last 400 years. The current C/N atomic ratio is slightly below 10, which suggests a higher algal production but TOC values are, in general, low indicating oligotrophic conditions. The C/N atomic ratio drops at ~300 cal. yr BP, and since then, there is a good correlation ($r = 0.84$, p-value <0.01) between $\delta^{13}C$ and Zr/Th ratios (Supplementary information). These factors suggest a strong biogeochemical response to aeolian Saharan input in the LdRS during this period. Moreover, the origin of the aeolian dust changes when comparing the La/Lu and the Zr/Th ratios. This is probably linked with the onset of commercial agriculture in the Sahel region in the last 200 years (Mulitza et al., 2010) and/or export of dust from new areas.

4.3. Cyclical changes driving Saharan aeolian input and regional effective humidity

Cyclostratigraphic studies show millennial- to centennial-scale variability in different Holocene climate proxy records (e.g., Bond et al., 2001; Debret et al., 2007). At LdRS we have obtained clearly ~2600–2200 yr and ~1500–1400 yr climate periodicities (Fig. 4). As discussed below, both periodicities have been related to solar activity and/or marine circulation characteristics, yet the interpretations remain controversial and the forcing mechanism not completely understood (e.g., Rahmstorf, 2003; Debret et al., 2007; Pena et al., 2010; Obrochta et al., 2012).

The 2600–2200 yr cycle is the most frequently registered cycle at LdRS, being observed in proxies of aeolian dust and redox conditions (La/Lu, Mn/Al, and $\delta^{13}C$). Mn/Al (dysoxic–anoxic conditions) and $\delta^{13}C$ signal indicate variations in humidity that also appear to affect the La/Lu ratio suggesting that recurrence of aeolian dust with different provenance or including new dust sources is also linked with aridity. Other Mediterranean marine and lacustrine sediments have also described similar periodicities (Kloosterboer-van Hoeve et al., 2006; Rodrigo-Gámiz et al., 2014). The 2600–2200 yr cycle has been described in high- and low-latitudes in both hemispheres linked with variations in solar activity and monsoonal variability (e.g., Sirocko, 1996; Nederbragt and Thurow, 2005; McGowan et al., 2010).

The 1500–1400 yr cycle is registered in proxies of runoff and effective humidity (Mg/Al and $\delta^{13}C$). This climate cycle has been persistently detected in the North Atlantic and Mediterranean climate regions (Bond et al., 1993; Moreno et al., 2005; Debret et al., 2007; Pena et al., 2010; Rodrigo-Gámiz et al., 2014) and has been linked with solar activity and oceanographic circulation. In any case, it has been demonstrated that North Atlantic Oscillation-like (NAO) variations control moisture penetration into the western Mediterranean (Trigo et al., 2004) at multi-decadal (Hurrel, 1995) to millennial scales (Moreno et al., 2005). The ~1500 yr cycle control the NAO-like intensity (Debret et al., 2007), the major forcing for the North Atlantic westerlies position and consequent penetration of winter storm tracks into the Mediterranean region (Thompson and Wallace, 2001). It is remarkable that $\delta^{13}C$ appears to be affected by both cycles. This could be related to the double nature of this proxy, affected by the biogeochemical changes in the lacustrine system linked with variations in aeolian dust as pointed out for the 2600–2200 yr cycle, but also with conditions of effective humidity, related to the water use efficiency in vascular plants (Farquhar et al., 1982) and algal development described at higher-frequency periodicities.

The 1500 yr cyclicity has also been related to aridity of dust source areas in western Africa and the intensity of dust transported by trade winds (deMenocal and Rind, 1993) but our dust proxies at LdRS do not appear to be sensitive to such cycles. The main connection with this cycle is the significant correlation (0.80) between La/Lu and Mg/Al ratios (Fig. 3 group IV) pointing newly to rainfall as major control in the dust source composition. The other dust proxies could be less sensitive because high altitude meridional dust transport is controlled by different mechanisms at this periodicity. All these evidences reinforce the strong link between solar irradiance and dust transport to LdRS most likely controlled by NAO-like variations for the millennial-scale cycles obtained.

4.4. Triggering atmospheric factors for Saharan dust input over Western Europe

Though our study indicates that solar irradiance and aridity modulated the cyclic dust influx to alpine area over westernmost Europe, our data also suggest that meridional dust transport mechanism appears to be different from long-range atmospheric transport in the Tropical region (Prospero and Lamb, 2003; Engelstaedter et al., 2006). The relationship between climatic changes in the Mediterranean region and atmospheric circulation in the northern Atlantic has also been demonstrated in previous studies (e.g., van Geel et al., 1996; Lamy et al., 2006; Magny et al., 2011 among others). In this sense, recent studies based on proxies of direct solar activity and models indicate that certain Holocene arid phases appear to be driven by amplified minor solar variations (Martin-Puertas et al., 2012). In any case, present day conditions indicate that various mechanisms could be related to the convection and/or trajectories of Saharan dust over the southern Iberia Peninsula:

(1) Dust convection requires Saharan low pressure development during summer over the North African Sahara, as a result of the intense surface heating. Additionally, an atmospheric upper level high creates a pressure gradient that bring dust to high altitudes (3–5 km) where it is transported over a wide area of the Mediterranean, including the Iberian Peninsula (Knippertz and Todd, 2012; Negral et al., 2012). At decadal scales solar intensity mainly changes in the ultraviolet field (5–8%), promoting disturbances at atmospheric middle altitudes that could be transferred to the lowest levels (Lean et al., 2005; Gray et al., 2010). Moreover, it has been described how Eastern North Atlantic Central Waters are very sensitive to minima in solar irradiance during NAO positive years (Morley et al., 2011). Both mechanisms could affect aridity and atmospheric conditions over western Africa by affecting the convection intensity.
(2) Meridional transport of Saharan dust that reached high altitudes (3–5 km) toward Europe requires specific atmospheric configurations. Dust is transported over south Iberia mainly when low-pressures are located in the Atlantic region and high pressures exist over the Central Mediterranean (e.g., Rodríguez et al., 2001), a probable configuration during summer–fall–winter. This kind of configuration could have been more common during NAO positive index periods when strong lows are located over the North Atlantic and strong subtropical high pressures dominate the Saharan–Mediterranean region (Trigo et al., 2004).

5. Conclusions

The LdRS deposits have preserved a clear and continuous record of aeolian dust deposition in southern Spain during the Holocene. During the early Holocene (~11.1–10.5 cal. kyr BP), the preserved arid signal results from the combination of atmospheric and glacier trapped Saharan dust. After this period, our data indicate that Saharan aridity, summer low pressure system intensity and required atmospheric configuration for meridional transport was punctually established from 7.0 to 6.1 cal. kyr BP, and persistently from 6.0 cal. kyr BP until present. During the last 400 years changes in the aeolian dust nature have been recognized. The arrival of dust promoted major biogeochemical changes on the lacustrine system reflected in the productivity.

Studied proxies indicate humid conditions and poorly oxygenated waters in the lake during the early Holocene. A major change took place at 6.0 cal. kyr BP when lake changed abruptly from primarily algal organic matter to a predominance of terrestrial vascular plants. From 6.0 cal. kyr BP until present a progressive increase in aridity in the region can be recognized, interrupted by rare periods of increasingly humid periods.

Cyclostratigraphic analysis indicates two main periodicities: at 2600–2200 yr, linked with dust input and redox proxies, and ~1500 yr cycles associated with changes in effective humidity. These two cycles suggest different forcing mechanisms that triggered paleoclimatic oscillations, both ultimately linked to solar activity and to NAO-like circulation the latest.

Supplementary data to this article can be found online at http://dx.doi.org/10.1016/j.chemgeo.2014.03.001.

Acknowledgements

Research was supported by Projects CGL2008-03007, CGL2012-32659 and CGL2012-33281 (Sec. Estado de I + D + I, Spain), Project RNM-3715 and Res. Groups RNM-178, RNM-179, RNM 5212 and RNM-190 (Junta Andalucía). Ministerio de Economía y Competitividad CGL BOS 2011.12909-E, CGL2010-20857/BTE y Min. Medio Ambiente y Medio Rural y Marino Proyecto 261/2011. The authors are indebted to Dr. M. Böttcher as editor and two anonymous reviewers for their invaluable comments and reviews. Our thanks to E. Holanda, C. Niembro, and D. Ortega for their laboratory assistance.

References

Aarons, S.M., Aciego, S.M., Gleason, J.D., 2013. Variable Hf–Sr–Nd radiogenic isotopic composition in a Saharan dust storm over the Atlantic: implications for dust flux to oceans, ice sheet and the terrestrial biosphere. Chem. Geol. 349–350, 18–26.
Adkins, J., deMenocal, P., Eshel, G., 2006. The "African humid period" and the record of marine upwelling excess ^{230}Th in Ocean Drilling Program Hole 658C. Paleoceanography 21. http://dx.doi.org/10.1029/2005PA001200 (PA4203).
Adrian, R., O'Reilly, C.M., Zagarese, H., Baines, S.B., Hessen, D.O., Keller, W., Livingstone, D.M., Sommaruga, R., Straile, D., Van Donk, E., Weyhenmeyer, A., Winder, M., 2009. Lakes as sentinels of climate change. Limnol. Oceanogr. 54, 2283–2297.
Allan, M., Le Roux, G., de Vleeschouwer, F., Bindler, R., Blaauw, M., Piotrowska, N., Sikorski, J., Fagel, N., 2013. High-resolution of atmospheric deposition of trace metals and metalloids since AD 1400 recorded by ombrotrophic peat cores in Hautes–Fagnes, Belgium. Environ. Pollut. 178, 381–394.
An, F.Y., Ma, H., Wei, H., Lai, Z., 2012. Distinguishing aeolian signature from lacustrine sediments of the Qaidam Basin in northeastern Qinghai–Tibetan Plateau and its palaeoclimatic implications. Aeolian Res. 4, 17–30.
Anderson, R.S., Jiménez-Moreno, G., Carrión, J., Pérez-Martinez, C., 2011. Postglacial history of alpine vegetation, fire, and climate from Laguna de Río Seco, Sierra Nevada, southern Spain. Quat. Sci. Rev. 30, 1615–1629.
Antón, M., Valenzuela, A., Cazorla, A., Gil, J.E., Fernández-Gálvez, J., Lyamani, H., Foyo-Moreno, I., Olmo, F.J., Alados-Arboledas, L., 2012. Global and diffuse shortwave irradiance during a strong desert dust episode at Granada (Spain). Atmos. Res. 118, 232–239.
Arbuszewski, J.A., deMenocal, P.B., Cléroux, C., Bradmiller, L., Mix, A., 2013. Meridional shifts of the Atlantic intertropical convergence zone since the Last Glacial Maximum. Nat. Geosci. 6, 959–962. http://dx.doi.org/10.1038/ngeo1961.
Bar-Matthews, M., Ayalon, A., Gilmour, M., Matthews, A., Hawkeswoth, C.J., 2003. Sea–land oxygen isotopic relationships from planktonic foraminifera and speleothems in the Eastern Mediterranean region and their implication for paleorainfall during interglacial intervals. Geochim. Cosmochim. Acta 67, 3181–3199.
Bea, F., 1996. Residence of REE, Y, Th and U in granites and crustal protoliths; implications for the chemistry of crustal melts. J. Petrol. 37, 521–552. http://dx.doi.org/10.1093/petrology/37.3.521.
Bellin, N., Vanacker, V., de Baets, S., 2013. Anthropogenic and climatic impact on Holocene sediment dynamics in SE Spain: a review. Quat. Int. http://dx.doi.org/10.1016/j.quaint.2013.03.015.
Berger, A., Loutre, M.F., 1991. Insolation values for the climate of the last 10 million years. Quat. Sci. Rev. 10, 297–317.
Bilali, L.E., Rasmussen, P.E., Hall, G.E.M., Fortin, D., 2002. Role of sediment composition in trace metal distribution in lake sediments. Appl. Geochem. 17, 1171–1181.
Blanchet, C.L., Tjallingii, R., Frank, M., Lorenzen, J., Reitz, A., Brown, K., Feseker, T., Brückmann, W., 2013. High- and low-latitude forcing of the Nile River regime during

the Holocene inferred from laminated sediments of the Nile deep-sea fan. Earth Planet. Sci. Lett. 364, 98–110.
Bond, G., Broecker, W.S., Johnsen, S.J., McManus, J., Labeyrie, L., Jouzel, J., Bonani, G., 1993. Correlations between climate records from North Atlantic sediments and Greenland ice. Nature 365, 143–147.
Bond, G., Kromer, B., Beer, J., Muscheler, R., Evans, M.N., Showers, W., Hoffmann, S., Lotti-Bond, R., Hajdas, I., Bonani, G., 2001. Persistent solar influence on North Atlantic climate during the Holocene. Science 294, 2130–2135.
Bonnet, S., Guieu, C., Chiaverini, J., Ras, J., Stock, A., 2005. Effect of atmospheric nutrients on the autotrophic communities in a low nutrient, low chlorophyll system. Limnol. Oceanogr. 50, 1810–1819.
Bozzano, G., Kuhlmann, H., Alonso, B., 2002. Stominess control over African dust input to the Moroccan Atlantic margin (NW Africa) at the time of maxima boreal summer insolation: a record of the last 220 kyr. Palaeogeogr. Palaeoclimatol. Palaeoecol. 183, 155–168.
Brumsack, H.J., 1986. The inorganic geochemistry of Cretaceos black shales (DSDP Leg 41) in compararison to modern upwelling sediments from the Gulf of California. In: Shackelton, N.J., Summerhayes, C.P. (Eds.), North Atlantic Paleoceanography: London. Geol. Soc. Special Publication, 21, pp. 447–462.
Calvert, S.E., Pedersen, T.F., 1993. Geochemistry of recent oxic and anoxic marine sediments: implications for the geological record. Mar. Geol. 113 (1–2), 67–88.
Calvert, S.E., Pedersen, T.F., 2007. Chapter fourteen elemental proxies for palaeoclimatic and palaeoceanographic variability in marine sediments: interpretation and application. In: Hillaire-Marcel, C., De Vernal, A. (Eds.), Proxies in Late Cenozoic Paleoceanography. Developments in Marine Geology. Elsevier, Oxford, UK, pp. 567–644.
Carrión, J.S., 2002. Patterns and processes of Late Quaternary environmental change in a montane region of southwestern Europe. Quat. Sci. Rev. 21, 2047–2066.
Carrión, J.S., Yll, E.I., Walker, M.J., Legaz, A.J., Chaín, C., López, A., 2003. Glacial refugia of temperate, Mediterranean and Ibero-North African flora in south-eastern Spain: new evidence from cave pollen at two Neanderthal man sites. Glob. Ecol. Biogeogr. 12, 119–129.
Castillo, S., Moreno, T., Querol, X., Alastuey, A., Cuevas, E., Herrmann, L., Mounkaila, M., Gibbons, W., 2008. Trace element variation in size-fractionated African desert dusts. J. Arid Environ. 72, 1034–1045.
Castillo Martín, A., 2009. Lagunas de Sierra Nevada. Editorial Universidad de Granada, Granada.
Cole, J.M., Goldstein, S.L., deMenocal, P.B., Hemming, S.R., Grousset, F.E., 2009. Contrasting compositions of Saharan dust in the eastern Atlantic Ocean during the last deglaciation and African Humid Period. Earth Planet. Sci. Lett. 278, 257–266.
Cortés-Sánchez, M., Morales-Muniz, A., Simon-Vallejo, M.D., Lozano-Francisco, M.C., Vera-Pelaez, J.L., Finlayson, C., Rodriguez-Vidal, J., Delgado-Huertas, A., Jimenez-Espejo, F.J., Martinez-Ruiz, F., Martinez-Aguirre, M.A., Pascual-Granged, A.J., Bergada-Zapata, M.M., Gibaja-Bao, J.F., Riquelme-Cantal, J.A., Lopez-Saez, J.A., Rodrigo-Gámiz, M., Sakai, S., Sugisaki, S., Finlayson, G., Fa, D.A., Bicho, N.F., 2011. Earliest known use of marine resources by Neanderthals. PLoS ONE 6, e24026. http://dx.doi.org/10.1371/journal.pone.0024026.
Cortés Sánchez, M., Jiménez Espejo, F.J., Simón Vallejo, M.D., Gibaja Bao, J.F., Faustino Carvalho, A., Martinez-Ruiz, F., Rodrigo Gámiz, M., Flores, J.A., Paytan, A., López Sáez, J.A., Peña-Chocarro, L., Carrión, J.S., Morales Muñiz, A., Roselló Izquierdo, E., Riquelme Cantal, J.A., Dean, R.M., Salgueiro, E., Martínez Sánchez, R.M., la Rubia, De, de Gracia, J.J., Lozano Francisco, M.C., Vera Peláez, J.L., Bicho, N.F., 2012. The Mesolithic–Neolithic transition in southern Iberia. Quat. Res. http://dx.doi.org/10.1016/j.yqres.2011.12.003.
Das, S.K., Routh, J., Roychoudhury, A.N., Klump, J.V., 2008. Major and trace element geochemistry in Zeekoevlei, South Africa: a lacustrine record of present and past processes. Appl. Geochem. 23, 2496–2511.
Debret, M., Bout-Roumazeilles, V., Grousset, F., Desmet, M., McManus, J.F., Massei, N., Sebag, D., Petit, J.-R., Copard, Y., Trentesaux, A., 2007. The origin of the 1500-year climate cycles in Holocene North-Atlantic records. Clim. Past 3, 569–575.
Debret, M., Sebag, D., Crosta, X., Massei, N., Petit, J.-R., Chapron, E., Bout-Roumazeilles, V., 2009. Evidence from wavelet analysis for a mid-Holocene transition in global climate forcing. Quat. Sci. Rev. 28, 2675–2688.
DeMenocal, P.B., Rind, D., 1993. Sensitivity of Asian and African climate to variations in seasonal insolation, glacial ice cover, sea surface temperatures, and Asian orography. J. Geophys. Res. 98, 7265–7287. http://dx.doi.org/10.1029/92JD02924.
deMenocal, P., Ortiz, J., Guilderson, T., Adkins, J., Sarnthein, M., Baker, L., Yarusinsky, M., 2000. Abrupt onset and termination of the African Humid Period: rapid climate responses to gradual insolation forcing. Quat. Sci. Rev. 19, 347–361.
R Development Core Team, 2013. R: A Language and Environment for Statistical Computing. available at: http://www.R-project.org ((last access: April 2013), R package version 2.13.0, 2011).
Diem, D., Stumn, W., 1984. Is dissolved Mn^{+2} being oxidized by O_2 in absence of Mn-bacteria or surface catalysts? Geochim. Cosmochim. Acta 48, 1571–1573.
Drysdale, R., Zanchetta, G., Hellstrom, J., Maas, R., Fallick, A., Pickett, M., Cartwright, I., Piccini, L., 2006. Late Holocene drought responsible for the collapse of Old World civilizations is recorded in an Italian cave flowstone. Geology 34, 101–104. http://dx.doi.org/10.1130/G22103.1.
Eglinton, T.I., Eglinton, G., Dupont, L., Sholkovitz, E.R., Montluçon, D., Reddy, C.M., 2002. Composition, age and provenance of organic matter in NW African dust over the Atlantic Ocean. Geochem. Geophys. Geosyst. 3 (8), GC000269.
Elbaz-Poulichet, F., Nagy, A., Cserny, T., 1997. The distribution of redox sensitive elements (U, As, Sb, V and Mo) along a river wetland lake system (Balaton Region, Hungary). Aquat. Geochem. 3, 267–282.
Engelstaedter, S., Tegen, I., Washington, R., 2006. North African dust emissions and transport. Earth Sci. Rev. 79, 73–100.
Erel, Y., Torrent, J., 2010. Contribution of Saharan dust to Mediterranean soils assessed by sequential extraction and Pb and Sr isotopes. Chem. Geol. 275, 19–25.
Eusterhues, K., Heinrichs, H., Schneider, J., 2005. Geochemical response on redox fluctuations in Holocene lake sediments, Lake Steisslingen, Southern Germany. Chem. Geol. 222, 1–22.
Farquhar, G.D., O'Leary, M.H., Berry, J.A., 1982. On the relationship between carbon isotope discrimination and the intercellular carbon dioxide concentration in leaves. Aust. J. Plant Physiol. 9, 121–137.
Fletcher, W.J., Sáncher Goñi, M.F., 2008. Orbital- and sub-orbital-scale climate impacts on vegetation of the western Mediterranean basin over the last 48,000 yr. Quat. Res. 70, 451–464.
Gallego-Torres, D., Martínez-Ruiz, F., Paytan, A., Jiménez-Espejo, F.J., Ortega-Huertas, M., 2007. Pliocene–Holocene evolution of depositional conditions in the eastern Mediterranean: role of anoxia vs. productivity at time of sapropel deposition. Palaeogeogr. Palaeoclimatol. Palaeoecol. 246, 424–439.
García-Alix, A., Jiménez-Moreno, G., Scott Anderson, R., Jimenez-Espejo, F.J., Delgado-Huertas, A., 2012. Holocene environmental change in southern Spain deduced from the isotopic record of a high-elevation wetland in Sierra Nevada. J. Paleolimnol. 48, 471–484.
García-Alix, A., Jimenez-Espejo, F.J., Lozano, J.A., Jiménez-Moreno, G., Martínez-Ruiz, F., García Sanjuan, L., Aranda Jiménez, G., García Alfonso, E., Ruiz-Puertas, G., Scott Anderson, R., 2013. Anthropogenic impact and lead pollution throughout the Holocene in Southern Iberia. Sci. Total Environ. 449, 451–460.
Goudie, A.S., Middleton, N.J., 2001. Saharan dust storms: nature and consequences. Earth Sci. Rev. 56, 179–204.
Govindaraju, K., 1994. Compilation of working values and sample description for 383 geostandards. Geostand. Newslett. 18, 1–158.
Gray, L., Beer, J., Geller, M., Haigh, J.D., Lockwood, M., Matthes, K., Cubasch, U., Fleitmann, D., Harrison, G., Hood, L., Luterbacher, J., Meehl, G.A., Shindell, D., van Geel, B., White, W., 2010. Solar influences on climate. Rev. Geophys. 48, RG4001.
Griffin, D.W., Kellogg, C.A., 2004. Dust storms and their impact on ocean and human health: dust in Earth's atmosphere. EcoHealth 1, 284–295. (0.1007/s10393-004-0120-8).
Guo, Z., Petit-Maire, N., Kröpelin, S., 2000. Holocene non-orbital climatic events in present-day arid areas of northern Africa and China. Global Planet. Chang. 26, 97–103.
Hamroush, H.A., Stanley, A.D.J., 1990. Paleoclimatic oscillations in East Africa interpreted by analysis of trace elements in Nile delta sediments. Episodes 13, 264–269.
Hemming, S.R., 2007. Terrigenous sediments. In: Elias, S.A. (Ed.), Encyclopedia of Quaternary Science, vol. 3. Elsevier, Oxford, pp. 1776–1785.
Hodell, D., Crowhurst, S., Skinner, L., Tzedakis, P.C., Margari, V., Channell, J.E.T., Kamenov, G., Maclachlan, S., Rothwell, G., 2013. Response of Iberian Margin sediments to orbital and suborbital forcing over the past 420 ka. Paleoceanography 28, 1–15. http://dx.doi.org/10.1029/2012PA002398.
Hurrel, J.W., 1995. Decadal trends in the North Atlantic Oscillation: regional temperatures and precipitation. Science 269, 676–679.
Jahns, S., 1993. On the Holocene vegetation history of the Argive Plain (Peloponnese, southern Greece). Veg. Hist. Archaeobot. 2, 187–203.
Jalut, G., Esteban Amat, A., Bonnet, L., Gauquelin, T., Fontugne, M., 2000. Holocene climatic changes in the Western Mediterranean, from south-east France to south-east Spain. Palaeogeogr. Palaeoclimatol. Palaeoecol. 160, 255–290.
Jalut, G., Dedoubat, J.J., Fontugne, M., Otto, T., 2011. Holocene circum-Mediterranean vegetation changes: climate forcing and human impact. Quat. Int. 200, 4–18.
Jimenez-Espejo, F.J., Martinez-Ruiz, F., Finlayson, C., Paytan, A., Sakamoto, T., Ortega-Huertas, M., Finlayson, G., Iijima, K., Gallego-Torres, D., Fa, D., 2007a. Climate forcing and Neanderthal extinction in Southern Iberia: insights from a multiproxy marine record. Quat. Sci. Rev. 26, 836–852.
Jimenez-Espejo, F.J., Martinez-Ruiz, F., Sakamoto, T., Iijima, K., Gallego-Torres, D., Harada, N., 2007b. Paleoenvironmental changes in the western Mediterranean since the last glacial maximum: high resolution multiproxy record from the Algero–Balearic basin. Palaeogeogr. Palaeoclimatol. Palaeoecol. 246, 292–306.
Jiménez-Moreno, G., Anderson, R.S., 2012. Holocene vegetation and climate change recorded in alpine bog sediments, Sierra Nevada, southern Spain. Quat. Res. 77, 44–53.
Jiménez-Moreno, G., García-Alix, A., Hernández-Corbalán, M.D., Anderson, R.S., Delgado-Huertas, A., 2013. Vegetation, fire, climate and human disturbance history in the southwestern Mediterranean area during the late Holocene. Quat. Res. 79, 110–122.
Jouve, G., Francus, P., Lamoureux, S., Provencher-Nolet, L., Hahn, A., Haberzettl, T., Fortina, D., Nuttin, L., 2013. Microsedimentological characterization using image analysis and μ-XRF as indicators of sedimentary processes and climate changes during Lateglacial at Laguna Potrok Aike, Santa Cruz, Argentina. Quat. Sci. Rev. http://dx.doi.org/10.1016/j.quascirev.2012.06.003.
Jung, S.J.A., Davies, G.R., Ganssen, G.M., Kroon, D., 2004. Stepwise Holocene aridification in NE Africa deduced from dust-borne radiogenic isotope records. Earth Planet. Sci. Lett. 221, 27–37.
Kloosterboer-van Hoeve, M.L., Steenbrink, J., Visscher, H., Brinkhuis, H., 2006. Millennial-scale climatic cycles in the Early Pliocene pollen record of Ptolemais, northern Greece. Palaeogeogr. Palaeoclimatol. Palaeoecol. 229, 321–334. http://dx.doi.org/10.1016/j.palaeo.2005.07. 002.
Knippertz, P., Todd, M.C., 2012. Mineral dust aerosols over the Sahara: meteorological controls on emission and transport and implications for modeling. Rev. Geophys. 50, RG1007. http://dx.doi.org/10.1029/2011RG000362.
Lamy, F., Arz, H.W., Bond, G.C., Bahr, A., Pätzold, J., 2006. Multicentennial-scale hydrological changes in the Black Sea and northern Red Sea during the Holocene and the Arctic/North Atlantic Oscillation. Paleoceanography 21, PA1008. http://dx.doi.org/10.1029/2005PA001184.

Lean, J., Rottman, G., Harder, J., Kopp, G., 2005. SORCE contributions to new understanding of global change and solar variability. Sol. Phys. 230, 27–53.
Lézine, A.-M., 2009. Timing of vegetation changes at the end of the Holocene Humid Period in desert areas at the northern edge of the Atlantic and Indian monsoon systems. Compt. Rendus Geosci. 341, 750–759.
Liu, Z., Wang, Y., Gallimore, R., Gasse, F., Johnson, T., deMenocal, P., Adkins, J., Notaro, M., Prentice, I.C., Kutzbach, J., Jacob, R., Behling, P., Wang, L., Ong, E., 2007. Simulating the transient evolution and abrupt change of Northern Africa atmosphere–ocean–terrestrial ecosystem in the Holocene. Quat. Sci. Rev. 26, 1818–1837.
Lomb, N.R., 1976. Least-squares frequency analysis of unequally spaced data. Astrophys. Space Sci. 39, 447–462.
Loÿe-Pilot, M.D., Martin, J.M., Morelli, J., 1986. Influence of Saharan dust on the rain acidity and atmospheric input to the Mediterranean. Nature 321, 427–428.
Mackereth, F.J.H., 1966. Some chemical observations on post-glacial lake sediments. Philos. Trans. R. Soc. Lond. B Biol. Sci. 250, 165–213.
Magny, M., Vannière, B., Calo, C., Millet, L., Leroux, A., Peyron, O., Zanchetta, G., La Mantia, T., Tinner, W., 2011. Holocene hydrological changes in south-western Mediterranean as recorded by lake-level fluctuations at Lago Preola, a coastal lake in southern Sicily, Italy. Quat. Sci. Rev. 30, 2459–2475.
Maher, B.A., Prospero, J.M., Mackie, D., Gaiero, D., Hesse, P.P., Balkanski, Y., 2010. Global connections between Aeolian dust, climate and ocean biogeochemistry at the present day and at the last glacial maximum. Earth Sci. Rev. 99, 61–97.
Mahowald, N.M., Zender, C.S., Luo, C., Savoie, D., Torres, O., del Corral, J., 2002. Understanding the 30-year Barbados desert dust record. J. Geophys. Res. 107, 4561. http://dx.doi.org/10.1029/2002JD002097.
Mangini, A., Jung, M., Laukenmann, S., 2001. What do we learn from peaks of uranium and of manganese in deep sea sediments? Mar. Geol. 177, 63–78.
Marshall, M.H., Lamb, H.F., Huws, D., Davies, S.J., Bates, R., Bloemendal, J., Boyle, J., Leng, M. J., Umer, M., Bryant, C., 2011. Late Pleistocene and Holocene drought events at Lake Tana, the source of the Blue Nile. Global Planet. Chang. 78, 147–161.
Martin-Puertas, C., Jiménez-Espejo, F., Martinez-Ruiz, F., Nieto-Moreno, V., Rodrigo, M., Mata, M.P., Valero-Garcés, B.L., 2010. Late Holocene climate variability in the south-western Mediterranean region: an integrated marine and terrestrial geochemical approach. Clim. Past 6, 807–816.
Martin-Puertas, C., Matthes, K., Brauer, A., Muscheler, R., Hansen, F., Petrick, C., Aldahan, A., Possnert, G., van Geel, B., 2012. Nat. Geosci. http://dx.doi.org/10.1038/ngeo1460.
Martinez-Ruiz, F., Kastner, M., Paytan, A., Ortega-Huertas, M., Bernasconi, S.M., 2000. Geochemical evidence for enhanced productivity during S1 sapropel deposition in the eastern Mediterranean. Paleoceanography 15, 200–209.
Marx, S.M., Kamber, B.S., McGowan, H.A., Denholm, J., 2011. Holocene dust deposition rates in Australia's Murray–Darling Basin record the interplay between aridity and the position of the mid-latitude westerlies. Quat. Sci. Rev. 30, 3290–3305.
Mathews, W.H., 1956. Physical limnology and sedimentation in a glacial lake. Geol. Soc. Am. Bull. 67, 537–552. http://dx.doi.org/10.1130/0016-7606.
McGowan, H.A., Marx, S.K., Soderholm, J., Denholm, J., 2010. Evidence of solar and tropical ocean forcing of hydroclimate cycles in southeastern Australia for the past 6500 years. Geophys. Res. Lett. 37, L10705. http://dx.doi.org/10.1029/2010GL042918.
Meyers, P.A., 1994. Preservation of elemental and isotopic source identification of sedimentary organic matter. Chem. Geol. 113, 289–302.
Meyers, P.A., Teranes, J.L., 2001. Sediment organic matter. In: Last, W.M., Smol, J.P. (Eds.), Tracking environmental changes using lake sediments, vol. 2. Kluwer, Dordrecht, pp. 239–270.
Mladenov, N., Sommaruga, R., Morales-Baquero, R., Laurion, I., Camarero, L., Diéguez, M.C., Camacho, A., Delgado, A., Torres, O., Chen, Z., Felip, M., Reche, I., 2011. Dust inputs and bacteria influence dissolved organic matter in clear alpine lakes. Nat. Commun. 2, 405. http://dx.doi.org/10.1038/ncomms1411.
Morales-Baquero, R., Carrillo, P., Reche, I., Sánchez-Castillo, P., 1999. Nitrogen–phosphorus relationship in high mountain lakes: effects of the size of catchment basins. Can. J. Fish. Aquat. Sci. 56, 1809–1817.
Morales-Baquero, R., Pulido-Villena, E., Reche, I., 2006. Atmospheric inputs of phosphorus and nitrogen to the Southwest Mediterranean region: biogeochemical responses of high mountain lakes. Limnol. Oceanogr. 51, 830–837.
Morales-Molino, C., García-Antón, M., Postigo-Mijarra, J.M., Morla, C., 2013. Holocene vegetation, fire and climate interactions on the westernmost fringe of the Mediterranean Basin. Quat. Sci. Rev. 59, 5–17.
Morellón, M., Valero-Garcés, B., Vegas-Vilarrúbia, T., González-Sampériz, P., Romero, Ó., Delgado-Huertas, A., Mata, P., Moreno, A., Rico, M., Corella, J.P., 2009. Lateglacial and Holocene palaeohydrology in the western Mediterranean region: the Lake Estanya record (NE Spain). Quat. Sci. Rev. 28, 2582–2599.
Moreno, A., Targarona, J., Henderiks, J., Canals, M., Freudenthal, T., Meggers, H., 2001. Orbital forcing of dust supply to the North Canary Basin over the last 250 kyrs. Quat. Sci. Rev. 20, 1327–1339.
Moreno, A., Cacho, I., Canals, M., Grimalt, J.O., Sánchez Goñi, M.F., Shackleton, N., Sierro, F.J., 2005. Links between marine and atmospheric processes oscillating on a millennial time-scale. A multi-proxy study of the last 50,000 yr from the Alboran Sea (Western Mediterranean Sea). Quat. Sci. Rev. 24, 1623–1636.
Moreno, A., López-Merino, L., Leira, M., Marco-Barba, J., González-Sampériz, P., Valero-Garcés, B., López-Sáez, J., Santos, L., Mata, P., Ito, E., 2011. Revealing the last 13,500Â years of environmental history from the multiproxy record of a mountain lake (Lago Enol, northern Iberian Peninsula). J. Paleolimnol. 46, 327–349.
Moreno, T., Querol, X., Castillo, S., Alastuey, A., Cuevas, E., Herrmann, L., Mounkaila, M., Elvira, J., Gibbons, W., 2006. Geochemical variations in aeolian mineral particles from the Sahara–Sahel Dust Corridor. Chemosphere 65, 261–270.
Morley, A., Schulz, M., Rosenthal, Y., Mulitza, S., Paul, A., Rühlemann, C., 2011. Solar modulation of North Atlantic central Water formation at multidecadal timescales during the late Holocene. Earth Planet. Sci. Lett. 308, 161–171.
Moulin, C., Lambert, C.E., Dulac, F., Dayan, U., 1997. Control of atmospheric export of dust from North Africa by the North Atlantic Oscillation. Nature 387, 691–694.
Mulitza, S., Heslop, D., Pittauerova, D., Fischer, H.W., Meyer, I., Stuut, J.-B., Zabel, M., Mollenhauer, G., Collins, J.A., Kuhnert, H., Schulz, M., 2010. Increase in African dust flux at the onset of commercial agriculture in the Sahel region. Nature 466, 8. http://dx.doi.org/10.1038/nature09213.
Mush, D.R., Budahn, J., Avila, A., Skipp, G., Freeman, J., Patterson, D., 2010. The role of African dust in the formation of Quaternary soils on Mallorca, Spain. Quat. Sci. Rev. 29, 2518–2543.
Mush, D.R., 2013. The geologic records of dust in the Quaternary. Aeolian Res. 9, 3–48. http://dx.doi.org/10.1016/j.aeolia.2012.08.001.
Naeher, S., Gilli, A., North, R., Hamman, Y., Schubert, C.J., 2013. Tracing bottom water oxygenation with sedimentary Mn/Fe ratios in Lake Zurich, Switzerland. Chem. Geol. 352, 125–133. http://dx.doi.org/10.1016/j.chemgeo.2013.06.006.
Negral, L., Moreno-Grau, S., Querol, X., Moreno, J., Viana, M., García-Sánchez, A., Alastuey, A., Moreno-Clavel, J., 2012. Weak pressure gradient over the Iberian Peninsula and African dust outbreaks: a new dust long transport scenario. Bull. Am. Meteorol. Soc. 1125–1132. http://dx.doi.org/10.1175/BAMS-D-10-05000.
Nederbragt, A.J., Thurow, J., 2005. Amplitude of ENSO cycles in the Santa Barbara Basin, off California, during the past 15 000 years. J. Quat. Sci. 20, 447–456. http://dx.doi.org/10.1002/jqs.946.
Niedermeyer, E.M., Schefuß, E., Sessions, A.L., Mulitza, S., Mollenhauer, G., Schulz, M., Wefer, G., 2010. Orbital- and millennial-scale changes in the hydrologic cycle and vegetation in the western African Sahel: insights from individual plant wax δD and $\delta^{13}C$. Quat. Sci. Rev. 29, 2996–3005.
Nieto-Moreno, V., Martínez-Ruiz, F., Giralt, S., Jiménez-Espejo, F.J., Gallego-Torres, D., Rodrigo-Gámiz, M., García-Orellana, J., Ortega-Huertas, M., de Lange, G.J., 2011. Tracking climate variability in the western Mediterranean during the Late Holocene: a multiproxy approach. Clim. Past 7, 635–675. http://dx.doi.org/10.5194/cpd-7-635-2011.
Obrochta, S.P., Miyahara, H., Yokoyama, Y., Crowley, T.J., 2012. A re-examination of evidence for the North Atlantic "1500-year cycle" at Site 609. Quat. Sci. Rev. 55, 23–33.
Och, L.M., Müller, B., Voegelin, A., Ulrich, A., Göttlicher, J., Steiniger, R., Mangold, S., Vologina, E.G., Sturm, M., 2012. New insights into the formation and burial of Fe/Mn accumulation in Lake Baikal sediments. Chem. Geol. 330–331, 244–259.
Oliva, M., Gómez-Ortiz, A., 2012. Late-Holocene environmental dynamics and climate variability in a Mediterranean high mountain environment (Sierra Nevada, Spain) inferred from lake sediments and historical sources. The Holocene 22, 915–927. http://dx.doi.org/10.1177/0959683611434235.
Ortiz, J.E., Torres, T., Delgado, A., Julià, R., Lucini, M., Llamas, F.J., Reyes, E., Soler, V., Valle, M. , 2004. The palaeoenvironmental and palaeohydrological evolution of Padul Peat Bog (Granada, Spain) over one million years, from elemental, isotopic and molecular organic geochemical proxies. Org. Geochem. 35, 1243–1260.
Ortiz, J.E., Torres, T., Delgado, A., Llamas, F.J., Soler, V., Valle, M., Julià, R., Moreno, L., Díaz-Bautista, A., 2010. Palaeoenvironmental changes in the Padul basin (Granada, Spain) over the last 1 Ma base on the biomarker content. Palaeogeogr. Palaeoclimatol. Palaeoecol. 298, 286–299.
Pena, L.D., Francés, G., Diz, P., Esparza, M., Grimalt, J.O., Nombela, M.A., Alejo, I., 2010. Climate fluctuations during the Holocene in NW Iberia: high and low latitude linkages. Cont. Shelf Res. 30, 1487–1496.
Palade, B., Palacios Estremera, D., Gomez Ortiz, A., 2011. Los glaciares rocosos de Sierra Nevada y su significado paleoclimático. Una primera aproximación. Cuad. Investig. Geogr. 37, 95–118.
Pardo-Igúzquiza, E., Rodríguez-Tovar, F.J., 2000. The permutation test as a non-parametric method for testing the statistical significance of power spectrum estimation in cyclostratigraphic research. Earth Planet. Sci. Lett. 181, 175–189.
Pardo-Igúzquiza, E., Rodríguez-Tovar, F.J., 2012. Spectral and cross-spectral analysis of uneven time series with the smoothed Lomb–Scargle periodogram and Monte Carlo evaluation of statistical significance. Comput. Geosci. 49, 207–216.
Petit-Maire, N., Guo, Z., 1996. Mise en evidénce de variations climatiques holocenes rapides en phase dans les déserts actuels de Chine et du Nord de l'Afrique. C. R. Acad. Sci. Paris 322, 847–851 (2a).
Piper, D.Z., Calvert, S.E., 2009. A marine biogeochemical perspective on black shale deposition. Earth Sci. Rev. 95 (1–2), 63–96.
Petherick, L.M., McGowan, H.A., Kamber, B.S., 2009. Reconstructing transport pathways for late Quaternary dust from eastern Australia using the composition of trace elements of long traveled dusts. Geomorphology 105, 67–79.
Pey, J., Pérez, N., Castillo, S., Viana, M., Moreno, T., Pandolfi, M., López-Sebastián, J.M., Alastuey, A., Querol, X., 2009. Geochemistry of regional background aerosols in the Western Mediterranean. Atmos. Res. http://dx.doi.org/10.1016/j.atmosres.2009.07.001.
Prospero, J.M., Lamb, P.J., 2003. African droughts and dust transport to the Caribbean: climate change implications. Science 302, 1024–1027.
Pulido-Villena, E., Reche, I., Morales-Baquero, R., 2005. Food web reliance on allochthonous carbon in two high mountain lakes with contrasting catchments: a stable isotope approach. Can. J. Fish. Aquat. Sci. 62, 2640–2648.
Pulido-Villena, E., Reche, I., Morales-Baquero, R., 2006. Significance of atmospheric inputs of calcium over the southwestern Mediterranean region: high mountain lakes as tools for detection. Global Biochem. Cycles 20, GB2012. http://dx.doi.org/10.1029/2005GB002662.
Rahmstorf, S., 2003. Timing of abrupt climate change: a precise clock. Geophys. Res. Lett. 30, 1510. http://dx.doi.org/10.1029/1003GL017115.

Reche, I., Ortega-Retuerta, E., Romera, O., Pulido-Villena, E., Morales-Baquero, R., Casamayor, E.O., 2009. Effect of Saharan dust inputs on bacterial activity and community composition in Mediterranean lakes and reservoirs. Limnol. Oceanogr. 54, 869–879.

Richardson, L.L., Nealson, K.H., 1989. Distributions of manganese, iron, and manganese oxidising bacteria in Lake Superior sediments of different organic carbon content. J. Great Lakes Res. 15, 123–132.

Rodríguez, S., Querol, X., Alastuey, A., Kallos, G., Kakaliagou, O., 2001. Saharan dust contributions to PM10 and TSP levels in Southern and Eastern Spain. Atmos. Environ. 35, 2433–2447.

Rodríguez-Tovar, F.J., Reolid, M., Pardo-Igúzquiza, E., 2010. Planktonic versus benthic foraminifera response to Milankovitch forcing (Late Jurassic, Betic Cordillera): testing methods for cyclostratigraphic analysis. Facies 56, 459–470.

Rodrigo-Gámiz, M., Martínez-Ruiz, F., Jiménez-Espejo, F.J., Gallego-Torres, D., Nieto-Moreno, V., Romero, O., Ariztegui, D., 2011. Impact of climate variability in the western Mediterranean during the last 20,000 years: oceanic and atmospheric responses. Quat. Sci. Rev. http://dx.doi.org/10.1016/j.quascirev.2011.05.011.

Rodrigo-Gámiz, M., Martínez-Ruiz, F., Rodríguez-Tovar, F.J., Jiménez-Espejo, F.J., Pardo-Igúzquiza, E., 2014. Millennial- to centennial-scale climate periodicities and forcing mechanisms in the westernmost Mediterranean for the past 20,000 yr. Quat. Res. http://dx.doi.org/10.1016/j.yqres.2013.10.009.

Rohling, E.J., Mayewski, P.A., Challenor, P., 2003. On the timing and mechanism of millennial-scale climate variability during the last glacial cycle. Clim. Dyn. 20, 257–267.

Rollinson, H., 1993. Using Geochemical Data: Evaluation, Presentation, Interpretation. Pearson Education Ltd., Edinburgh.

Sadori, L., Narcisi, B., 2001. The Postglacial record of environmental history from Lago di Pergusa, Sicily. The Holocene 11, 655–670.

Sadori, L., Ortu, E., Peyron, O., Zanchetta, G., Vannière, B., Desmet, M., Magny, M., 2013. The last 7 millennia of vegetation and climate changes. Clim. Past 9, 2059–2094.

Scargle, J.D., 1982. Studies in astronomical time series analysis. II. Statistical aspects of spectral analysis of unevenly spaced data. Astrophys. J. 263, 835–853.

Schaller, T., Wehrli, B., 1996. Geochemical focusing of manganese in lake sediments — an indicator of deep-water oxygen conditions. Aquat. Geochem. 2, 359–378.

Scheuvens, D., Schütz, L., Kandler, K., Ebert, M., Weinbruch, S., 2013. Bulk composition of northern African dust and its source sediments — a compilation. Earth-Sci. Rev. 116, 170–194.

Schulte, L., 2002. Climatic and human influence on river systems and glacier fluctuations in southeast Spain since the Last Glacial Maximum. Quat. Int. 93–94, 85–100.

Shinn, E.A., Smith, G.W., Prospero, J.M., Betzer, P., Hayes, M.L., Garrison, V., Barber, R.T., 2000. African dust and the demise of Caribbean coral reefs. Geophys. Res. Lett. 27, 3029–3032.

Shotyk, W., Krachler, M., Martinez-Cortizas, A., Cheburkin, A.K., Emons, H., 2002. A peat bog record of natural, pre-anthropogenic enrichments of trace elements in atmospheric aerosols since 12 370 ^{14}C yr BP, and their variation with Holocene climate change. Earth Planet. Sci. Lett. 199, 21–37.

Skonieczny, C., Bory, A., Bout-Roumazeilles, V., Abouchami, W., Galer, S.J.G., Crosta, X., Diallo, A., Ndiaye, T., 2013. A three-year time series of mineral dust deposits on the West African margin: sedimentological and geochemical signatures and implications for interpretation of marine paleo-dust records. Earth Planet. Sci. Lett. 364, 145–156.

Sirocko, F., 1996. Past and present subtropical summer monsoons. Science 274, 937–938. http://dx.doi.org/10.1126/science.274.5289.937.

Stuiver, M., Reimer, P.J., Bard, E., Beck, J.W., Burr, G.S., Hughen, K.A., Kromer, B., McCormac, F.G., Plicht, J., Spurk, M., 1998. INTCAL98 radiocarbon age calibration 24,000–0 cal BP. Radiocarbon 40, 1041–1083.

Suzuki, R., Shimodaira, H., 2011. Pvclust: hierarchical clustering with p-values via multiscale bootstrap resampling. R package version 1.2–2 (http://CRAN.R-project.org/package=pvclust).

Talbot, R.W., Harriss, R.C., Browell, E.V., Gregory, G.L., Sebacher, D.I., Beck, S.M., 1986. Distribution and geochemistry of aerosols in the tropical north Atlantic troposphere: relationship to Saharan dust. J. Geophys. Res. 91, 5173–5182.

Thompson, D.W.J., Wallace, J.M., 2001. Regional climate impacts of the northern hemisphere annular mode. Science 293, 85–89.

Thompson, L.G., Mosley-Thompson, E., Davis, M.E., Henderson, K.A., Brecher, H.H., Zagorodnov, V.S., Mashiotta, T.A., Lin, P.N., Mikhalenko, V.N., Hardy, D.R., Beer, J., 2002. Kilimanjaro ice core records: evidence of Holocene climate change in tropical Africa. Science 298, 589–593.

Trauth, M.H., Larrasoaña, J.C., Mudelsse, M., 2009. Trends, rhythms and events in Plio-Pleistocene African climate. Quat. Sci. Rev. 28, 399–411.

Trigo, R.M., Pozo-Vázquez, D., Osborn, T.J., Castro-Díez, Y., Gámiz-Fortis, S., Esteban-Parra, M.J., 2004. North Atlantic oscillation influence on precipitation, river flow and water resources in the Iberian Peninsula. Int. J. Climatol. 24, 925–944. http://dx.doi.org/10.1002/joc.1048.

Van der Weijden, C.H., 2002. Pitfalls of normalization of marine geochemical data using a common divisor. Mar. Geol. 184, 167–187.

van Geel, B., Buurman, J., Waterbolk, H.T., 1996. Archaeological and palaeoecological indications of an abrupt climate change in The Netherlands, and evidence for climatological teleconnections around 2650 BP. J. Quat. Sci. 11, 451–460.

Versteegh, G.J.M., de Leeuw, Taricco, C., Romero, A., 2007. Temperature and productivity influences on $U^{K'}_{37}$ and their possible relation to solar forcing of the Mediterranean winter. Geochem. Geophys. Geosyst. 8, Q09005. http://dx.doi.org/10.1029/2006GC001543.

Waeles, M., Alex, R., Baker, A.R., Jickells, T., Hoogewerff, J., 2007. Global dust teleconnections: aerosol iron solubility and stable isotope composition. Environ. Chem. 4, 233–237.

Wehausen, R., Brumsack, H.-J., 1999. Cyclic variations in the chemical composition of eastern Mediterranean Pliocene sediments: a key for understanding sapropel formation. Mar. Geol. 153, 161–176.